Microbead-Induced Ocular Hypertensive Mouse Model for Screening and Testing of Aqueous Production Suppressants for Glaucoma

Qiang Yang,[1,2,8] *Kin-Sang Cho,*[2,8] *Huihui Chen,*[2,3] *Dekuang Yu,*[2,4] *Wan-Heng Wang,*[5] *Gang Luo,*[2] *Iok-Hou Pang,*[5] *Wenyi Guo,*[*,1,6,8] *and Dong Feng Chen*[*,2,7,8]

Purpose. To characterize the microbead-induced ocular hypertension (OHT) mouse model and investigate its potential use for preclinical screening and evaluation of ocular hypotensive agents, we tested the model's responses to major antiglaucoma drugs.

Methods. Adult C57BL/6J mice were induced to develop OHT unilaterally by intracameral injection of microbeads. The effects of the most commonly used ocular hypotensive drugs, including timolol, brimonidine, brinzolamide, pilocarpine, and latanoprost, on IOP and glaucomatous neural damage were evaluated. Degeneration of retinal ganglion cells (RGCs) and optic nerve axons were quantitatively assessed using immunofluorescence labeling and histochemistry. Thickness of the ganglion cell complex (GCC) was also assessed with spectral-domain optical coherence tomography (SD-OCT).

Results. A microbead-induced OHT model promptly responded to drugs, such as timolol, brimonidine, and brinzolamide, that lower IOP through suppressing aqueous humor production and showed improved RGC and axon survival as compared to vehicle controls. Accordingly, SD-OCT detected significantly less reduction of GCC thickness in mice treated with all three aqueous production suppressants as compared to the vehicle contol–treated group. In contrast, drugs that increase aqueous outflow, such as pilocarpine and latanoprost, failed to decrease IOP in the microbead-induced OHT mice.

Conclusions. Microbead-induced OHT mice carry dysfunctional aqueous outflow facility and therefore offer a unique model that allows selective screening of aqueous production suppressant antiglaucoma drugs or for studying the mechanisms regulating aqueous humor production. Our data set the stage for using GCC thickness assessed by SD-OCT as an imaging biomarker for noninvasive tracking of neuronal benefits of glaucoma therapy in this model. (*Invest Ophthalmol Vis Sci.* 2012;53:3733–3741) DOI:10.1167/iovs.12-9814

The inducible mouse model of glaucoma is receiving increasing attention because of the advancement of mouse genetic technology, which has offered a powerful tool that can lead to molecular insights into the complex nature of the disease. Elevation of IOP is a well-recognized risk factor for glaucoma. Recently, a highly effective and reproducible method to induce IOP elevation in rodents by intracameral injection of microbeads has been developed.[1–4] Injection of microbeads to the mouse anterior chamber induced sustained IOP elevation and retinal ganglion cell (RGC) and axon degeneration, which simulates glaucomatous changes in human patients without causing apparent clinical signs of inflammation or overt damage in the anterior segment.[1–3] The model is rapidly gaining popularity because of its convenience, reliability, and minimum damage to ocular structures. The relatively low cost, as well as similar anatomical characteristics of the anterior segment, aqueous production, and outflow facility between rodent and human have also made the mouse an ideal animal model of experimental glaucoma for evaluation of potential treatments.[5–8] However, as microbeads obstruct the aqueous humor outflow, it remains unclear how these mice respond to ocular hypotensive drugs and whether they present a suitable model for preclinical testing and screening of glaucoma therapy.

A critical unmet need in using animal models to predict clinical success of a medicine and translating animal studies to bedside for glaucoma therapy is the development of surrogate measures of retinal neuron damage that allow direct comparison between animal and human. Recent advances in the development of high-resolution spectral-domain optical coherence tomography (SD-OCT) and its applicability to small rodents have made this possible. The nerve fiber layer (NFL) thickness assessed by OCT has been established as an essential measurement for objective glaucoma assessment in a clinic.[9–11] Recent studies indicate that the combined thickness of the NFL, ganglion cell layer (GCL), and inner plexiform layer (IPL),

From the [1]Department of Ophthalmology, Eye & ENT Hospital, Fudan University, Shanghai, P. R. China; the [2]Schepens Eye Research Institute, Massachusetts Eye and Ear, Department of Ophthalmology, Harvard Medical School, Boston, Massachusetts; the [3]Department of Ophthalmology, The Second Xiangya Hospital, Central South University, Changsha, Hunan, P. R. China; the [4]Biomedical Engineering School, Southern Medical University, Guangzhou, P. R. China; [5]Glaucoma Research, Alcon Research, Ltd., Fort Worth, Texas; the [6]Department of Ophthalmology, Ninth People's Hospital, Shanghai JiaoTong University School of Medicine, Shanghai, P. R. China; and the [7]Veterans Affairs Boston Healthcare System, Boston, Massachusetts.

[8]These authors contributed equally to the work presented here and should therefore be regarded as equivalent authors.

Supported by grants from NIH/NEI (R01EY017641), the Department of Veterans Affairs (1I01RX000110), the Department of Defense (W81XWH-09-2-0091), Alcon Fund (DFC), and the Science and Technology Commission of Shanghai Municipality 114119a7300 (WYG).

Submitted for publication March 7, 2012; revised May 11, 2012; accepted May 11, 2012.

Disclosure: **Q. Yang**, None; **K.-S. Cho**, None; **H. Chen**, None; **D. Yu**, None; **W.-H. Wang**, Alcon (E); **G. Luo**, None; **I.-H. Pang**, Alcon (E); **W. Guo**, None; **D.F. Chen**, Alcon (F)

*Each of the following is a corresponding author: Dong Feng Chen, Schepens Eye Research Institute, 20 Staniford Street, Boston, MA 02114; dongfeng.chen@schepens.harvard.edu.

Wenyi Guo, Department of Ophthalmology, Ninth People's Hospital, Shanghai JiaoTong University School of Medicine, Shanghai, P. R. China; wyguo@163.com.

together defined as the ganglion cell complex (GCC), also shows a comparable diagnosis capability with NFL thickness.[12,13] Previously, we and others have reported that NFL and GCC thickness show a close correlation with RGC axon degeneration in mouse models of acute optic nerve injury,[14–16] making them potential imaging biomarkers to link the animal work with a clinical readout for optic nerve damage. However, the key question remains whether NFL or GCC thickness assessed by SD-OCT can serve as a surrogate measure for RGC and axon degeneration in the microbead-induced OHT mouse model, in which loss of RGCs and axons may be moderate compared to the acute optic nerve injury models.[14–16] Moreover, we do not know whether injected microbeads would reduce topical transparency of the cornea or interfere with SD-OCT imaging of the retina.

In the present study, we investigated the potential of using microbead-induced OHT mice for preclinical testing of ocular hypotensive drugs by evaluating their responses to major antiglaucoma medications. In general, ocular hypotensive eye drops are broadly divided into two groups according to the mechanisms of actions: The first group comprises β-adrenoceptor antagonists (e.g., timolol), α1-adrenoceptor agonists (e.g., brimonidine), and carbonic anhydrase inhibitors (e.g., brinzolamide), which lower IOP by decreasing the rate of aqueous humor production. The second group includes prostaglandin FP receptor agonists (e.g., latanoprost) and muscarinic receptor agonists (e.g., pilocarpine), which reduce IOP by increasing aqueous humor outflow.[17] We selected the most commonly used eye drops from each group and investigated their capacities to lower IOP and prevent glaucomatous neurodegeneration in the microbead-induced OHT mouse model. Moreover, we conducted SD-OCT imaging and carried out correlative studies for quantification of RGC degeneration and GCC thickness assessed using custom-generated automated segmentation of SD-OCT images. Our studies established the feasibility of using the microbead-induced OHT mouse model for preclinical testing of glaucoma drugs and application of SD-OCT in this model for surrogate measures of neural damage and treatment efficacies.

Materials and Methods

Animals

All animal experiments were performed in accordance with the Association of Research for Vision and Ophthalmology Statement for the Use of Animals in Ophthalmic and Vision Research, and all protocols were reviewed and approved by the Animal Care and Use Committee at the Schepens Eye Research Institute. Adult C57BL/6J mice (8 to 12 weeks) used in this study were purchased from the Jackson Laboratory (Bar Harbor, ME). All animals were maintained on a 12 h light/12 h dark cycle (lights on at 6:00 AM) with food and water available ad libitum.

Induction of Elevated IOP

Mice were anesthetized by intraperitoneal injection of a mixture of ketamine (100 mg/kg; Ketaset; Fort Dodge Animal Health, Fort Dodge, IA) and xylazine (9 mg/kg; TranquiVed; Vedco, Inc., St. Joseph, MO) supplemented by topical application of proparacaine (0.5%; Bausch & Lomb, Tampa, FL). Elevation of IOP was induced unilaterally by injection of polystyrene microbeads (FluoSpheres; Invitrogen, Carlsbad, CA; 15-μm diameter) to the anterior chamber of the right eye of each animal under a surgical microscope, as previously reported.[3] Briefly, microbeads were reformulated at a concentration of 5.0×10^6 beads/mL in PBS. The right cornea was gently punctured near the center using a sharp glass micropipette (World Precision Instruments Inc., Sarasota, FL). A small volume (2 μL) of microbeads was injected through this preformed hole into the anterior chamber followed by injection of an air bubble via the micropipette connected with a Hamilton syringe. Mice were placed on a heating pad for recovery after the injection, and antibiotic Vetropolycin ointment (Dechra Veterinary Products, Overland Park, KS) was applied topically onto the injected eye to prevent infection. In most cases, the procedure did not induce clinical signs of ocular inflammation (e.g., opaque cornea or edema, iris exudation) when examined by slit lamp. However, 3 out of 75 injected mice showed signs of inflammation and were excluded from the study.

IOP Measurement

Mice were anesthetized by isoflurane inhalation (2%–4%; Webster Veterinary, Sterling, MA), which was delivered in 95% oxygen with a precision vaporizer. IOP measurement was initiated within 2 to 3 min after animals lost toe pinch reflex and blink reflex. IOP was measured with a TonoLab rebound tonometer (Colonial Medical Supply, Franconia, NH), which automatically generated a mean of six measurements after elimination of the highest and lowest values. This machine-generated mean was considered as one reading, and six readings were obtained from each eye. The means of six readings were calculated to determine the mean IOP. Baseline IOPs were obtained the day before microbead injection. To reflect cumulative exposure to the elevated IOP over time in each animal, cumulative IOP was calculated by multiplying the means of IOPs with the number of days after the drug treatment (mm Hg·days).

Drug Administration

Five ocular hypotensive drugs were used in this study. They were Isopto Carpine (2% pilocarpine hydrochloride ophthalmic solution; Alcon, Fort Worth, TX), timolol maleate (0.5% timolol; Merck & Co., Inc., Whitehouse Station, NJ), brimonidine tartrate (0.15%; Falcon Pharmaceuticals, Fort Worth, TX), Azopt (1% brinzolamide, Alcon), and Xalatan (0.005% latanoprost, Pfizer Pharmacia, Woodstock, IL). At 7 days after microbead injection, mouse eyes that developed significant elevation of IOP were topically treated with test drugs. For single-dose studies, a single dose (4 μL) of either the vehicle control (the Azopt formulation minus brinzolamide) or one of the five ocular hypotensive drugs was applied to the right eyes of mice between 8:00 and 11:00 AM, using a pipette. Mouse IOPs were measured before and at 1, 2, 6, and 24 hours after administration of the drug or the vehicle control. For repeated-dosing studies, mice received eye drops of either the vehicle control or one of the five ocular hypotensive drugs twice daily (9:00 AM and 5:00 PM, respectively) consecutively for up to 2 weeks beginning from 7 days postinjection of microbeads. Mouse IOPs were measured twice daily immediately before each administration of the eye drop, and daily IOP value was represented as the average of the two measurements.

RGC Quantification

RGC loss was assessed in retinal flat-mounts of both microbead-injected and noninjected contralateral eyes in groups treated with repeated dosing. Retinas were dissected and fixed in 4% paraformaldehyde (Boston Bioproducts, Ashland, MA) overnight. Retinal flat-mounts were flattened on SuperFrost Plus slides (VWR, Batavia, IL) and treated with 0.1% Triton and 2% fetal BSA in PBS for 1 hour, followed by incubation with a primary antibody against an RGC-specific marker, β-III-Tubulin (Tuj1; Millipore, Billerica, MA), overnight and a Cy3-conjugated secondary antibody (Jackson ImmunoResearch Laboratories, West Grove, PA) for 2 hours. Retinas were coverslipped with mounting medium (Vectashield; Vector Lab, Burlingame, CA) and imaged under the Leica TSC SP5 confocal microscope. The midperipheral area of the retina (~2 mm from the optic nerve head) was divided into eight distinct areas across all quadrants, and all Tuj1 positive (indicated as +) cells were counted. The percentage of RGC loss was calculated by

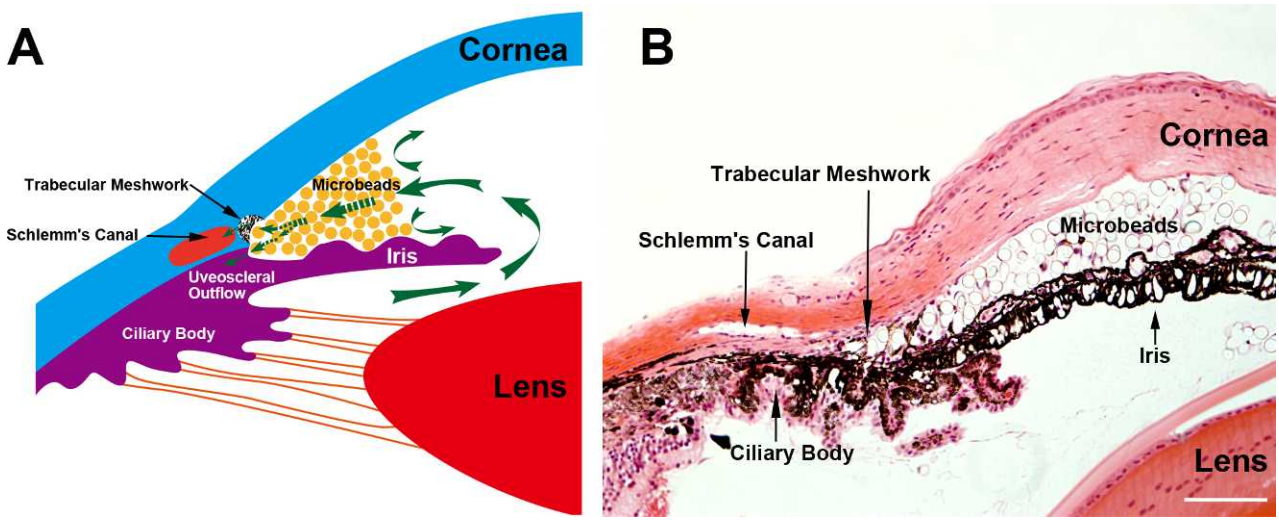

Figure 1. Microbead distribution in the mouse anterior chamber following intracameral injection. (**A**) Illustration of the iridocorneal angle structure: injected microbeads are accumulated at the iridocorneal angle that blocks both the uveoscleral and trabecular outflow pathways. (**B**) Representative photomicrograph of hematoxylin and eosin–stained eye sections taken from a mouse 7 days after microbead injection showing similar structure and microbead distribution as illustrated in (**A**). Scale bar: 100 μm.

dividing the number of RGCs counted from the microbead-injected eyes by the number from their contralateral noninjected control eyes. Quantification was performed in a double-masked manner.

Optic Nerve Axon Quantification

Optic nerves were harvested and fixed in 2.5% formaldehyde/2.5% glutaraldehyde at 4°C. Semithin optic nerve cross sections (0.75–1.0 μm) were stained by 1% *p*-phenylenediamine (Fisher Scientific Co., Fair Lawn, NJ) and imaged with a Nikon 90i microscope (Nikon Inc., Melville, NY) equipped with automated stage, Cool Snap HQ digital camera, and Nikon Elements software. A custom-generated program written in Nikon Elements was used to select the best section for high-resolution imaging at 10× or 20×. The program automatically scanned the selected sections at 100× oil objective to capture a digital montage of the entire nerve. Thirty such images were collected for a given nerve section. Using Nikon elements, each 100× image was processed to segment myelinated nerve axons as single objects for counting. For a given nerve, the total axon count was calculated by summing the counts of individual images.

SD-OCT Live Imaging

Mice were anesthetized with an intraperitoneal injection of a mixture of ketamine (100 mg/kg) and xylazine (9 mg/kg) and were kept warm on a heating blanket. Pupils were dilated with a topically applied eye drop of tropicamide (1%; Falcon Pharmaceuticals, Fort Worth, TX). Radial volumetric images, centered on the optic nerve head, were acquired from both eyes with a SD-OCT system (Bioptigen, Inc., Durham, NC). The Bioptigen OCT was designed for small animals and provided a high resolution of 2 μm. SD-OCT images of each eye consisted of 1000 A-scans × 100 B-scans, covering 50° field-of-view of the mouse retina. GCC thickness within a donut-shaped area centered at the optic nerve disc was measured for each Z-stack image pixel, resulting in a topographic GCC thickness map. The inner and outer radiuses of the donut-shaped area were 200 and 500 μm from the center of the optic nerve disc, respectively. This sampling area was chosen because the thickness in the area was relatively constant and therefore could provide a clearly defined measure. After the boundaries of GCC were identified from each B-scan, the custom software program we developed calculated the perpendicular distance between the two boundaries to yield a thickness value for B-scans. The mean GCC thickness for each eye was calculated by averaging the thickness values of 100 B-scans. Immediately after OCT, mice were euthanized, and eyes were collected for histological quantification for RGC and axon counts as described above. All of the analyses were carried out in a double-masked fashion.

Statistical Analysis

The effects of the ocular hypotensive agents were analyzed by comparing the treated groups and the vehicle control group using ANOVA, followed by Bonferroni's test. A P value <0.05 was considered statistically significant. All data are presented as mean ± SEM.

Results

IOP-Lowering Effects by a Single Dosing

To investigate the response of microbead-induced OHT mice to ocular hypotensive drugs, we evaluated the IOP-lowering effects of five of the most commonly used antiglaucoma eye drops. These included suppressants of aqueous humor production, namely, timolol, brimonidine, and brinzolamide, and drugs that increase the aqueous humor outflow, latanoprost and pilocarpine. To induce IOP elevation unilaterally, the right eye of each mouse received an anterior chamber injection of polystyrene microbeads. The contralateral eyes served as noninjected controls. Immediately following the injection, microbeads were distributed throughout the anterior chamber but gradually accumulated at the iridocorneal angle, which resulted in a blockade of both the uveoscleral and trabecular outflow pathways (Fig. 1). As we previously reported, IOP reached the plateau at about day 7 postinjection (mean IOP = 22.1 ± 0.5 mm Hg; $n = 48$) (data not shown).[3] At day 7, the mice were randomly assigned to one of the treatment groups and were administered with a single dose of either a vehicle control or one of the ocular hypotensive eye drops to the right eye. The levels of IOPs were measured before and at 1, 2, 6, and 24 hours after administration of the drug or vehicle control.

Topical application of the vehicle control did not cause significant changes in the mouse IOP (Fig. 2A). In contrast, three aqueous production suppressants, timolol (Fig. 2B), brimonidine (Fig. 2D), and brinzolamide (Fig. 2F), significantly

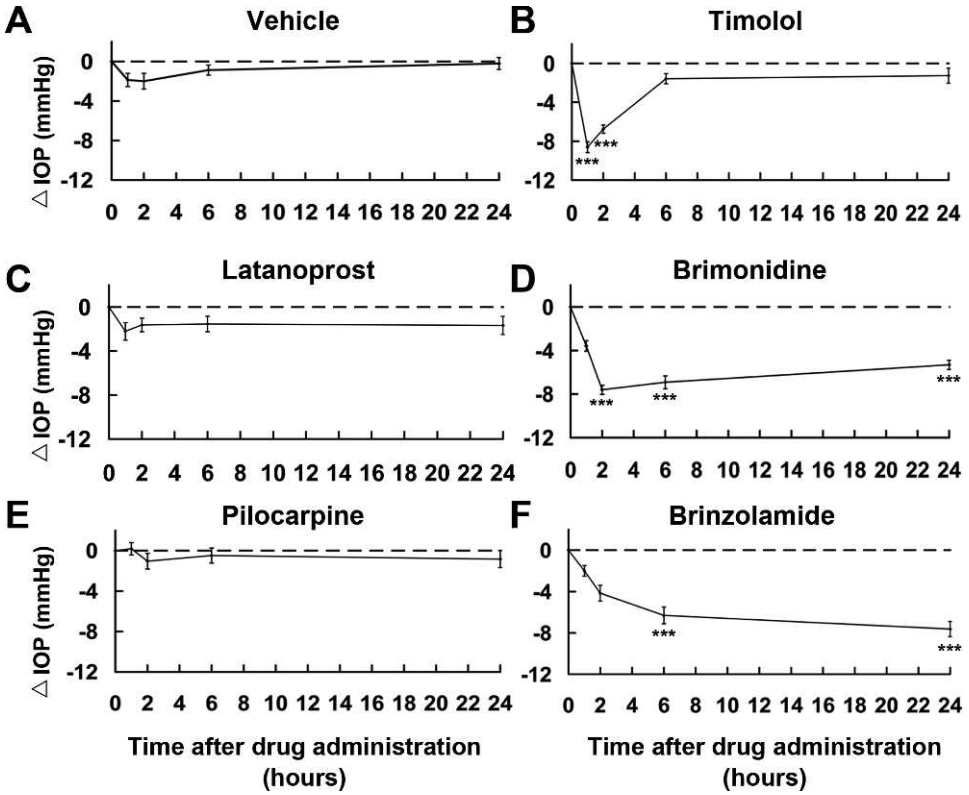

Figure 2. Short-term effects of a single dose of ocular hypotensive agents on microbead-induced OHT in mouse. A single eye drop was administered to the mouse right eye on day 7 after intracameral injection of microbeads. (**A**) Vehicle. (**B**) Timolol. (**C**) Latanoprost. (**D**) Brimonidine. (**E**) Pilocarpine. (**F**) Brinzolamide. Measurements of IOPs were conducted at 1, 2, 6, and 24 hours, respectively, after the administration of the eye drops or vehicle. $^{*}P < 0.05$; $^{**}P < 0.01$ as compared to the vehicle control–treated group by one-way ANOVA and Bonferroni's test (values are means ± SEM; $n = 8$/group).

lowered the IOP in the OHT eyes as compared to the vehicle control–treated group (Fig. 2A). These three drugs exhibited patterns of IOP-lowering kinetics similar to those seen in humans and monkeys.[18] A single dose of timolol reduced IOP by 8.6 ± 0.6 mm Hg at the peak between 1 and 2 hours postadministration of the drug, which returned to the baseline by ~6 hours; whereas, both brimonidine (peak reduction = 7.6 ± 0.4 mm Hg) and brinzolamide (peak reduction = 7.6 ± 0.7 mm Hg) induced significant IOP reduction that lasted over 24 hours. These data support the notion that the mouse has anatomical and functional characteristics of the anterior segment and aqueous production mechanisms similar to those of primates.[5–8] Interestingly, topical application of latanoprost (Fig. 2C) and pilocarpine (Fig. 2E) showed no significant effect on the microbead-induced OHT in mice at all time points examined. It has been shown that latanoprost effectively reduces normal IOP in naïve C57BL/6J mice.[19] We showed that administration of pilocarpine in naïve C57BL/6J mice also significantly lowered IOP from its baseline level (see Supplementary Fig. 1, http://www.iovs.org/lookup/suppl/doi:10.1167/iovs.12-9814/-/DCSupplemental). Moreover, the presence of microbeads in the OHT model did not impede the contractility of the ciliary muscles, as administration of pilocarpine consistently induced centripetal movement of the ciliary body (data not shown). These data suggest that the outflow facilities of C57BL/6J mice are equipped with the receptors and signaling transduction machinery required for responding to latanoprost and pilocarpine. Failure of latanoprost and pilocarpine to reduce IOP in the microbead-induced OHT mouse model suggests that the function of the ocular outflow facility in the OHT mice is disrupted. We conclude that the microbead-induced OHT mouse presents an effective model system for preclinical testing aimed at selection of suppressants of aqueous humor production. Its dysfunctional ocular outflow facility may offer a unique opportunity for the study of mechanisms or identification of drugs regulating aqueous production.

IOP-Lowering Effects by Repeated Dosing

To further evaluate the long-term effects of aqueous production suppressants, microbead-injected mice were administered with timolol, brimonidine, brinzolamide, or vehicle controls twice daily for up to 2 weeks, starting from day 7 postinjection of microbeads. Mouse IOPs were measured twice daily before each administration of the eye drops. As previously reported, the mouse IOP reached the peak on day 7 postinjection but gradually declined thereafter.[3] The animals were randomly assigned into each group, and mice of each group displayed similar IOPs before they began to receive eye drops (see Supplementary Fig. 2, http://www.iovs.org/lookup/suppl/doi:10.1167/iovs.12-9814/-/DCSupplemental). As expected, daily administration of the vehicle control did not have any short- or long-term effect on the mouse IOP as compared to mice that received no treatment (data not shown). The progressive decline in IOP levels in the vehicle control–treated group was a result of the gradual removal of microbeads from the aqueous outflow pathways (e.g., the iridocorneal angle structure and Schlemm's canal), either by flushing away or being phagocytized by adjacent cells.[3] Administration of timolol resulted in a reduction of IOP by 2.2 ± 0.1 mm Hg on average when compared to the vehicle control–treated

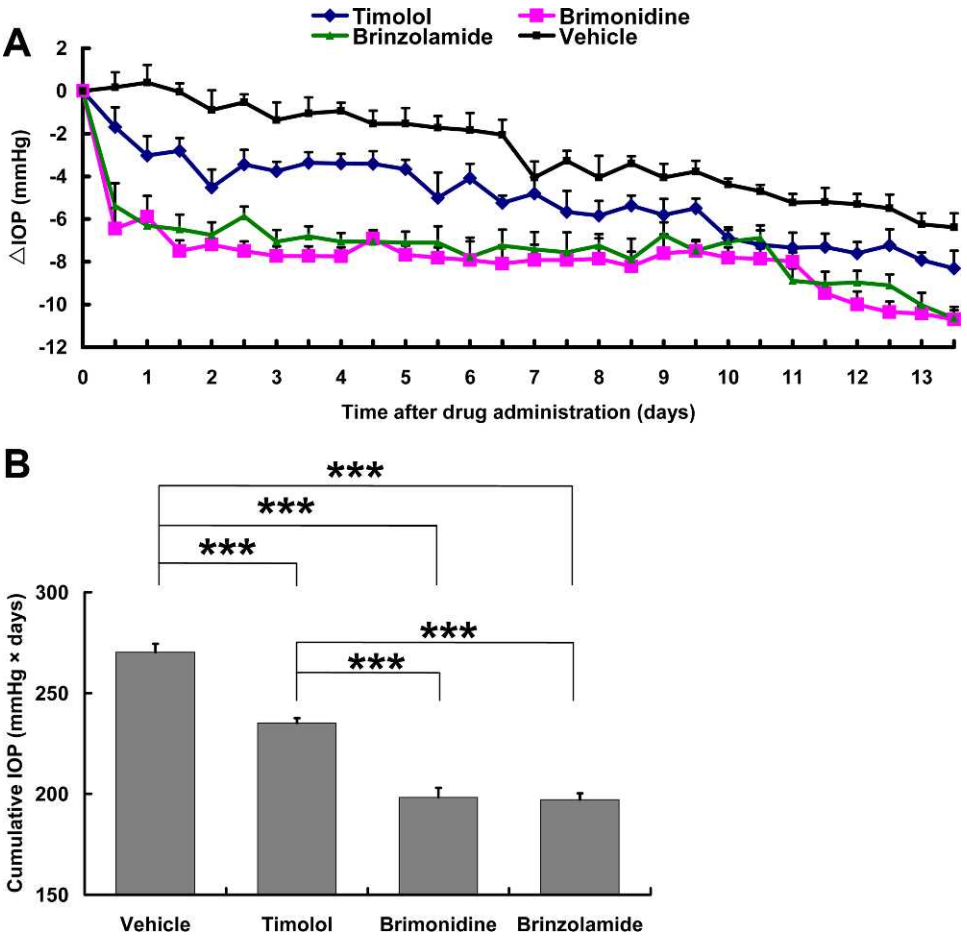

Figure 3. Longer-term effects of repeated dosing of ocular hypotensive agents on microbead-induced OHT in mice. Beginning at day 7 postinjection of microbeads, mice received either a vehicle control or one of the three aqueous production suppressants twice daily for 2 weeks consecutively. (**A**) Plot of daily IOP change assessed twice daily immediately before each application of eye drops. (**B**) Cumulative IOP during the 2-week treatment period. $^{***}P < 0.001$ as compared among the indicated groups by one-way ANOVA and Bonferroni's test (values are means ± SEM; $n = 6$/group).

group. Administration of repeated dosing of brimonidine and brinzolamide, however, led to a more constant and steady level of IOP reduction by 5.0 ± 0.3 mm Hg and 4.4 ± 0.2 mm Hg, respectively, throughout the period compared to the vehicle control–treated group (Fig. 3A). To better indicate the long-term IOP-lowering effect of the drugs, we calculated cumulative IOPs from each mouse (Fig. 3B). Data collected throughout the 2-week treatment period (days 8 to 21 postinjection of microbeads) showed that administration of all three aqueous production suppressants significantly reduced the levels of cumulative IOP as compared to the vehicle control–treated group, and that the cumulative IOPs of brimonidine- and brinzolamide-treated groups were significantly lower than those treated by timolol (Fig. 3B). Together, brimonidine and brinzolamide have a superior IOP-reducing effect over the longer term in the microbead-induced OHT mice. This result is in agreement with results reported in glaucoma patients.[20,21]

RGC and Axonal Survival

To evaluate the protective effects of IOP reduction on RGC and optic nerve axon degeneration, microbead-induced OHT mice were euthanized at 2 weeks after drug treatment. Loss of RGCs was determined quantitatively in retinal flat-mounts that were immunolabeled with an RGC-specific marker Tuj1.[3] Consistent with the IOP-lowering effects of the drugs, counts of Tuj1+ cells indicated that all three drug-treated groups exhibited significantly less RGC loss than did the vehicle control–treated group (Fig. 4). In comparison with 50.9% ± 3.5% of RGC loss in the vehicle control–treated group, the timolol-treated group displayed 29.8% ± 5.4% of RGC loss, while the brimonidine- and brinzolamide-treated groups exhibited 21.7% ± 3.7% and 24.2% ± 4.2% of RGC loss, respectively. Although both the brimonidine- and brinzolamide-treated groups tended to show improved RGC survival as compared to the timolol-treated group, we did not detect significant differences between them. This conclusion was confirmed by axon counts in semithin optic nerve cross sections using histochemistry and a computer-aided automated program. Two weeks of consecutive administration of timolol, brimonidine, or brinzolamide resulted in significant reduction of axon degeneration in drug-treated groups as compared to vehicle control–treated groups (Fig. 5). They exhibited 21.2% ± 9.6%, 17.4% ± 8.9%, and 19.0% ± 7.2% of axon loss, respectively, as compared to 57.8% ± 5.2% axon loss in the vehicle control–treated group. Together, these data show a close correlation between the IOP-lowering effect of the aqueous production suppressants and improvement of RGC and axon survival in the microbead-induced OHT mouse model.

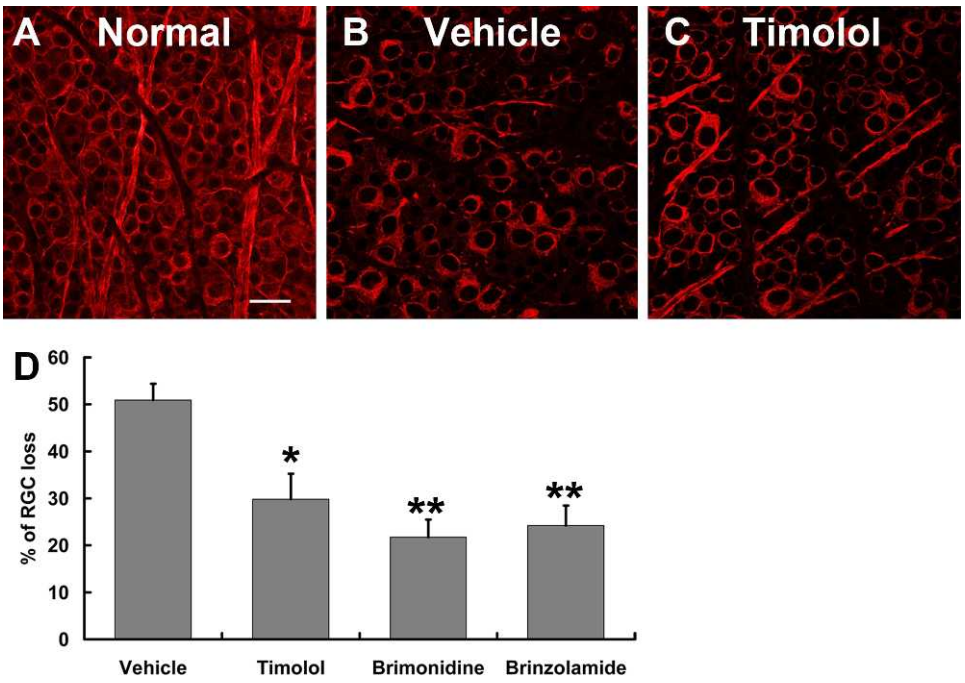

Figure 4. Quantification of RGC loss in mice. (**A–C**) Representative epifluorescence photomicrographs of retinal flat-mounts taken from the intermediate region of the retina from an uninjected control eye (**A**) and microbead-injected eyes that were treated twice daily for 2 weeks with either vehicle control (**B**) or timolol (**C**). RGCs were revealed by immunolabeling with a primary antibody against an RGC-specific marker Tuj1 (*red*). Scale bar: 20 μm. (**D**) Quantification of RGC loss after 2 weeks of consecutive administration of vehicle control or aqueous production suppressant eye drops. $^{*}P < 0.05$; $^{**}P < 0.01$ as compared to vehicle-treated group by one-way ANOVA and Bonferroni's test (values are means ± SEM; $n = 6$/group).

Concordance of RGC Loss with the Reduction of GCC Thickness

To determine whether SD-OCT can be used in the microbead-induced OHT mouse model to evaluate therapeutic efficacies of drug treatment, we measured the GCC thickness before mice were sacrificed for retinal histology. Thickness of the GCC, rather than NFL, was assessed in the present study, in part because NFL is very thin in mice and difficult to resolve by the software. More importantly, the GCC is composed of the NFL and GCL, where RGC soma reside, and IPL, which is occupied in large part by RGC dendrites, all of which are expected to be affected by glaucoma.[22–24] Radial scans centered on the optic nerve head were acquired from both eyes of mice with SD-OCT (Figs. 6A–D). Each layer of the retina in the mice, including the NFL and GCC, was clearly visualized in SD-OCT images (Fig. 6E). The existence of microbeads in the anterior chamber did not interfere with the clarity and assessment of retinal layers by SD-OCT. We found no apparent difference in the clarity of the images and scan morphology between the microbead-injected and noninjected eyes (data not shown). The en face and GCC superimposed SD-OCT images of both injected and noninjected eyes revealed similarly uninterrupted retinal structure and blood vessels (Figs. 6C, 6D).

To allow unbiased measure of GCC thickness in SD-OCT images, we developed a custom-generated software that automatically collected 100 radial scans from each eye and calculated the mean GCC thickness based on segmentation of a circular area ranging from 200 to 500 μm in diameter from the center of the optic nerve head (Figs. 6C, 6D). The retinal blood vessel pattern was distinctive on the thickness map and correlated with the pattern observed in the SD-OCT Z-stack en face fundus images displayed in grayscale (Figs. 6A, 6B). This validated the ability of the custom-generated program to accurately track the contours of retinal layers. The GCC thickness map of the microbead-induced OHT mouse retinas was whitish in color when compared to that of the control retina, indicating phenotypical thinning of the GCC in the OHT retinas (white color represents decreased thickness in color coding). Quantification of the GCC thickness showed a strong correlation between its reduction and RGC loss from histological analysis ($R^2 = 0.6453$; Fig. 6F). In accordance with the histology data, analysis of SD-OCT images consistently revealed less reduction in GCC thickness in the eyes of mice that received 2 weeks of consecutive administration of aqueous production suppressants than in those of the vehicle control group (Fig. 6G). While we calculated 10.0% ± 0.7% reduction of GCC thickness in the vehicle control–treated group, we noted only 3.0% ± 0.9% reduction of GCC thickness in the timolol-treated group. Consistently, we also noted a tendency of greater protective effects on GCC thickness induced by brimonidine and brinzolamide treatment as compared to timolol; brimonidine- and brinzolamide-treated groups showed 2.3% ± 1.6% and 1.0% ± 0.3% reduction of GCC thickness, respectively (Fig. 6G). Together, these data establish the applicability of SD-OCT for noninvasive monitoring of retinal histology and a close correlation between histology quantification of RGC degeneration and reduction of GCC thickness in the microbead-induced OHT mouse model.

Discussion

In this study, we have further characterized the newly developed microbead-induced mouse model of glaucoma. We report here that these mice display selective defects in the outflow facility of aqueous humor and offer a unique model system for preclinical testing of aqueous production suppres-

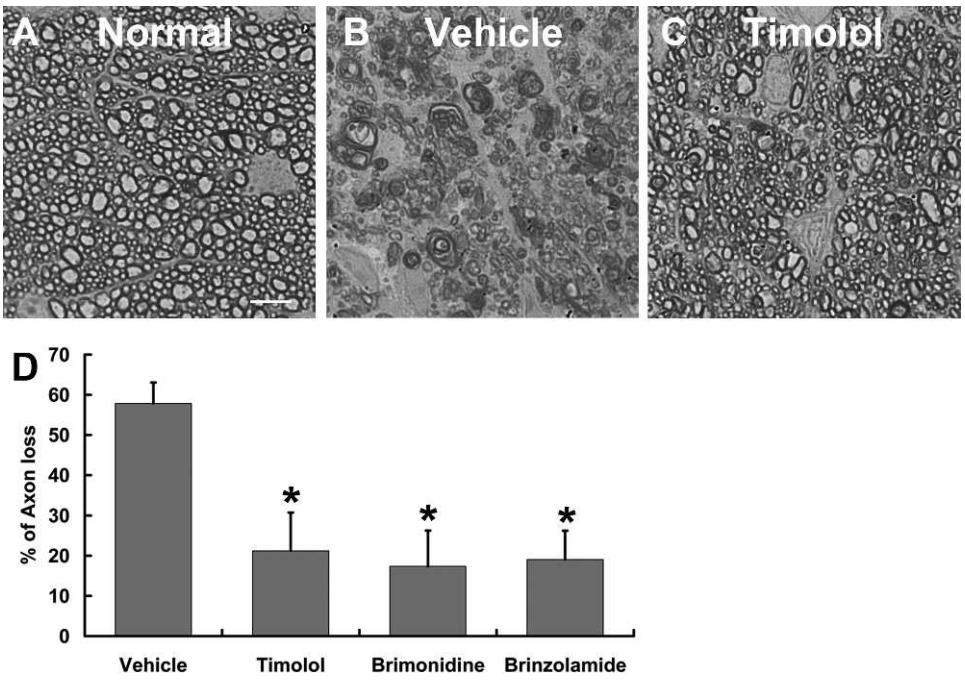

Figure 5. Quantification of optic nerve axon loss in mice. (**A–C**) Photomicrographs of EM images taken from *p*-phenylenediamine–stained optic nerve sections of an uninjected control eye (**A**) or microbead-injected eye that was treated twice daily for 2 weeks with either vehicle control (**B**) or timolol (**C**). Scale bar: 5 μm. (**D**) Quantification of axon loss after 2 weeks of consecutive administration of vehicle control or aqueous production suppressant eye drops. $^*P < 0.05$ as compared to vehicle control–treated group by one-way ANOVA and Bonferroni's test (values are means ± SEM; $n = 6$/group).

sants and the study of the mechanisms that control aqueous humor production. Moreover, we have developed an automated OCT image processing program that enables unbiased assessment of GCC and retinal layer thickness. We have demonstrated a strong correlation between the reduction of GCC thickness and histological quantification of RGC loss in the microbead-induced OHT mouse model. Thus, GCC thickness assessed by SD-OCT may serve as a reliable imaging biomarker for noninvasive and real-time tracking and quantification of glaucomatous neurodegeneration and for evaluation of the therapeutic efficacy of antiglaucoma drugs in live mice. The establishment of this method provides a surrogate measure of neuronal damage that allows direct comparison between the animal model and human glaucoma patients.

Specifically, we would like to point out that while microbead-induced OHT generally provides a convenient method for inducing glaucoma in mice, phenotypically, these mice imitate more closely the clinical conditions of pseudoexfoliation glaucoma and ghost cell glaucoma.[25–27] Pseudoexfoliation syndrome is an age-related disease of the extracellular matrix characterized by an accumulation of fibrillar exfoliation material in the ocular tissue[28] and is thought to be the most common identifiable cause of secondary open-angle glaucoma.[29] In this disease, OHT is attributed, at least partly, to the obstruction of conventional trabecular meshwork outflow; however, markedly reduced uveoscleral flow is also found in eyes with pseudoexfoliations.[30] Ghost cell glaucoma is another recently described glaucoma caused by vitreous hemorrhage, in which red blood cells degenerate into ghost cells and obstruct the trabecular meshwork.[31] Although ghost cell glaucoma is thought to be infrequent, a recent study indicates an increased incidence following intravitreal injection of bevacizumab for treating proliferating diabetic retinopathy.[32] In the microbead-induced OHT mice, the trabecular meshwork and uveoscleral pathways are severely obstructed. Therefore, the model may be even more valuable for understanding the pathogenesis of pseudoexfoliation and ghost cell glaucoma and for preclinical testing of drug therapies that target these clinical conditions.

Our results also indicate that aqueous production suppressants, such as brimonidine and brinzolamide, have a superior IOP-lowering effect on microbead-induced OHT, while antiglaucoma drugs targeting the aqueous humor outflow facility are ineffective under these conditions. Timolol, brimonidine, brinzolamide, pilocarpine, and latanoprost are five commonly used hypotensive drugs. Previous studies and our data demonstrated that these five agents effectively reduce normal IOP in naïve mice,[19,33,34] suggesting that mouse eyes are equipped with the receptors and pathways capable of responding to these eye drops. However, in the microbead-induced OHT model, topical administration of timolol, brimonidine, and brinzolamide, but not pilocarpine or latanoprost, produced significant IOP-lowering effects. In the single-dose studies, the IOP-lowering effect of timolol was short-lived, which observation is consistent with the reported fast clearance of the drug in human patients.[21,35] In contrast, brimonidine and brinzolamide showed a prominent effect on IOP reduction from 2 hours onward and lasted to 24 hours in microbead-induced OHT mice. This kinetic is also in agreement with that observed in humans.[21,35] Concordantly, brimonidine and brinzolamide exhibited a superior IOP-lowering effect as compared to timolol in the repeated-dosing studies (Fig. 3). In conclusion, aqueous production suppressant eye drops may represent an effective IOP-lowering therapy for treating pseudoexfoliation and ghost cell glaucoma.

Other ocular hypotensive drugs tested, latanoprost, which functions by enhancing uveoscleral outflow, and pilocarpine, which acts directly on the cholinergic parasympathetic pathway to open up the trabecular meshwork and facilitate the aqueous humor outflow, showed no effect on microbead-induced OHT. Together, these data are in agreement with the observation that the trabecular meshwork and entry of the

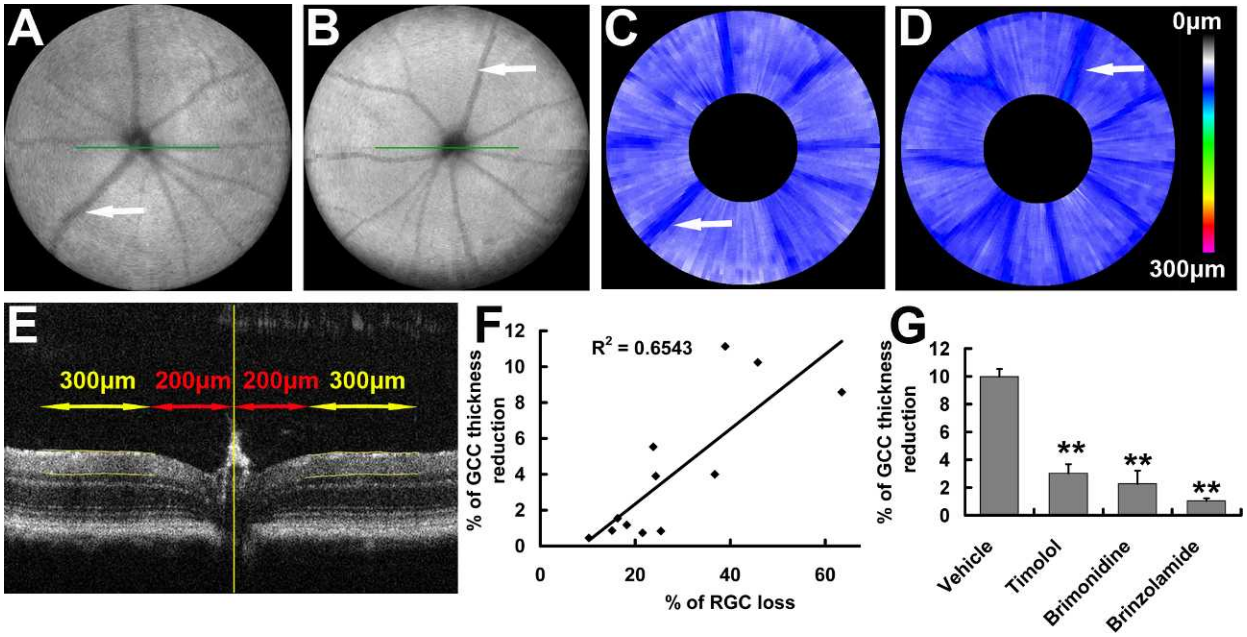

Figure 6. SD-OCT assessment of GCC thickness in mice. (**A**, **B**) SD-OCT en face images taken from a microbead-injected eye that was treated with vehicle control eye drops for 2 weeks consecutively (**A**) and its contralateral uninjected eye (**B**). (**C**, **D**) Colored GCC thickness map superimposed onto the SD-OCT en face images taken from those in **A** and **B**, respectively. The GCC thickness map of the microbead-injected mouse retina (**C**) was shifted toward a white color when compared to that of the contralateral normal retina (**D**), indicating phenotypical thinning of the GCC in the glaucoma retina as compared to the control retina. The retinal blood vessel pattern was distinctive and correlated with the pattern observed in (**A**, **B**). Arrows point to the blood vessels. (**E**) Representative retinal B-scan showing segmentation of SD-OCT image taken from an uninjected normal eye. The border lines (*yellow*) of the GCC layer were marked by a custom-generated automated program. (**F**) Correlation between the reduction of GCC thickness assessed by SD-OCT images and quantification of RGC loss measured from retinal flat-mounts ($R^2 = 0.6543$). (**G**) Percentage change of GCC thickness after 2 weeks of consecutive treatment of vehicle control or aqueous suppressant eye drops. $^{**}P < 0.01$ as compared to vehicle-treated group by one-way ANOVA and Bonferroni's test (values are means ± SEM; $n = 6$/group).

uveoscleral system are largely congested by the microbeads (Fig. 1), which results in complete dysfunction of the outflow facility in these mice. Alternatively, it is possible that the presence of microbeads in the iridocorneal angle and Schlemm's canal may also impact the mechanisms of actions of latanoprost and pilocarpine. For example, it has been shown that latanoprost lowers IOP through inducing endogenous PG synthesis in a dose-dependent manner.[36] Intracameral injection of microbeads may induce a maximal level of endogenous PG synthesis, which can further contribute to the failure of latanoprost to reduce IOP. While a primary mechanism of pilocarpine's function is to facilitate aqueous outflow by inducing ciliary muscle contraction, we noted that the presence of microbeads did not impede this capacity of pilocarpine. However, it is likely that contraction of ciliary muscle, while it may increase aqueous outflow under normal conditions, can facilitate the movement of microbeads and increase the number of beads that enter Schlemm's canal, resulting in further blockade of the trabecular meshwork. In any case, dysfunctional outflow facility in the microbead-induced OHT model may indeed offer a unique opportunity for studying the mechanisms that control aqueous humor production and for selection of drugs acting through this specific pathway.

It is worth noting that, in the present study, we adopted new procedures for RGC and axon quantification: First, we sampled the midperipheral retinal area for RGC counts while excluding the far peripheral and central retina. According to the previous reports,[3] RGC counts from the midperipheral retina generate more consistent results that better reflect the average loss of RGCs in the glaucoma mouse model than counts obtained from either the far peripheral or central retina. This was further proved by axon counts, in which we used a computer-generated automatic program that counts all axons in an entire optic nerve cross section. While in theory this new method should generate less biased and more accurate data on axon loss, interestingly, the results revealed more moderate axon damage than was documented previously in the glaucoma mouse model. A likely explanation is that the computer-generated program recognized only healthy and myelinated axons but excluded the degenerating and demyelinated ones in glaucomatous optic nerve sections. In the future, detailed analysis to understand the difference would be worthwhile. Together, our results support the notion that microbead-induced OHT is effective at inducing not only IOP elevation but also glaucomatous RGC and axon degeneration.

Another key finding in the present study is the establishment of the feasibility of using SD-OCT for quantitative measures of retinal layer thickness in real-time in the microbead-induced OHT mouse model. We and others have reported previously that reduction in NFL and GCC thickness shows a strong correlation with RGC axon degeneration in mouse models of acute optic nerve injury.[14–16] The results of our current study showed the utility of custom-generated automated segmentation of SD-OCT images in determining GCC thickness in the microbead-induced OHT mouse model. This methodology can be used in the future to characterize the temporal relationship between thinning of the inner retinal layers and cell loss at multiple time points during the progression of glaucoma. The correlation between the RGC counts and GCC thickness validates segmentation of SD-OCT imaging of retinal layers as a marker for glaucomatous neural damage in vivo. Further analysis of a 3D thickness map may generate more valuable information on topographical cell loss in association with the disease. These studies thus represent an important step in verifying the imaging capability of SD-OCT

for monitoring noninvasively and assessing quantitatively neuronal damage in glaucoma mouse models. Given that mice are the most commonly used and most powerful model system for studying the mechanism and preclinical testing of drug therapeutics, this effort will help to translate the animal work into clinical application for both diagnosing and evaluating efficacies of drugs for treating glaucoma.

References

1. Sappington RM, Carlson BJ, Crish SD, Calkins DJ. The microbead occlusion model: a paradigm for induced ocular hypertension in rats and mice. *Invest Ophthalmol Vis Sci*. 2010;51:207–216.
2. Cone FE, Gelman SE, Son JL, Pease ME, Quigley HA. Differential susceptibility to experimental glaucoma among 3 mouse strains using bead and viscoelastic injection. *Exp Eye Res*. 2010;91:415–424.
3. Chen H, Wei X, Cho KS, et al. Optic neuropathy due to microbead-induced elevated intraocular pressure in the mouse. *Invest Ophthalmol Vis Sci*. 2011;52:36–44.
4. Wei X, Yu Z, Cho KS, et al. Neuroglobin is an endogenous neuroprotectant for retinal ganglion cells against glaucomatous damage. *Am J Pathol*. 2011;179:2788–2797.
5. Lindsey JD, Weinreb RN. Identification of the mouse uveoscleral outflow pathway using fluorescent dextran. *Invest Ophthalmol Vis Sci*. 2002;43:2201–2205.
6. Smith RS, Zabaleta A, Savinova OV, John SW. The mouse anterior chamber angle and trabecular meshwork develop without cell death. *BMC Dev Biol*. 2001;1:3.
7. Aihara M, Lindsey JD, Weinreb RN. Aqueous humor dynamics in mice. *Invest Ophthalmol Vis Sci*. 2003;44:5168–5173.
8. Aihara M, Lindsey JD, Weinreb RN. Effect on diurnal intraocular pressure variation of eliminating the alpha-2 adrenergic receptor subtypes in the mouse. *Invest Ophthalmol Vis Sci*. 2008;49:929–933.
9. Wollstein G, Schuman JS, Price LL, et al. Optical coherence tomography longitudinal evaluation of retinal nerve fiber layer thickness in glaucoma. *Arch Ophthalmol*. 2005;123:464–470.
10. Schuman JS, Hee MR, Arya AV, et al. Optical coherence tomography: a new tool for glaucoma diagnosis. *Curr Opin Ophthalmol*. 1995;6:89–95.
11. Pagliara MM, Lepore D, Balestrazzi E. The role of OCT in glaucoma management. *Prog Brain Res*. 2008;173:139–148.
12. Tan O, Chopra V, Lu AT, et al. Detection of macular ganglion cell loss in glaucoma by Fourier-domain optical coherence tomography. *Ophthalmology*. 2009;116:2305–2314.
13. Strouthidis NG, Grimm J, Williams GA, Cull GA, Wilson DJ, Burgoyne CF. A comparison of optic nerve head morphology viewed by spectral domain optical coherence tomography and by serial histology. *Invest Ophthalmol Vis Sci*. 2010;51:1464–1474.
14. Camp AS, Ruggeri M, Munguba GC, et al. Structural correlation between the nerve fiber layer and retinal ganglion cell loss in mice with targeted disruption of the Brn3b gene. *Invest Ophthalmol Vis Sci*. 2011;52:5226–5232.
15. Nakano N, Hangai M, Nakanishi H, et al. Macular ganglion cell layer imaging in preperimetric glaucoma with speckle noise-reduced spectral domain optical coherence tomography. *Ophthalmology*. 2011;118:2414–2426.
16. Gregory MS, Hackett CG, Abernathy EF, et al. Opposing roles for membrane bound and soluble Fas ligand in glaucoma-associated retinal ganglion cell death. *PLoS One*. 2011;6:e17659.
17. Pang I-H, Clark AF. IOP as a target—inflow and outflow pathways. In: Yorio T, Clark AF, Wax MB, eds. *Ocular Therapeutics: An Eye on New Discoveries*. New York, NY: Academic Press; 2008:45–67.
18. Liu G, Zeng T, Yu W, et al. Characterization of intraocular pressure responses of the Tibetan monkey (Macaca thibetana). *Mol Vis*. 2011;17:1405–1413.
19. Husain S, Whitlock NA, Rice DS, Crosson CE. Effects of latanoprost on rodent intraocular pressure. *Exp Eye Res*. 2006;83:1453–1458.
20. van der Valk R, Webers CA, Schouten JS, Zeegers MP, Hendrikse F, Prins MH. Intraocular pressure-lowering effects of all commonly used glaucoma drugs: a meta-analysis of randomized clinical trials. *Ophthalmology*. 2005;112:1177–1185.
21. McKinnon SJ, Goldberg LD, Peeples P, Walt JG, Bramley TJ. Current management of glaucoma and the need for complete therapy. *Am J Manag Care*. 2008;14:S20–S27.
22. Wang X, Tay SS, Ng YK. An electron microscopic study of neuronal degeneration and glial cell reaction in the retina of glaucomatous rats. *Histol Histopathol*. 2002;17:1043–1052.
23. Kotera Y, Hangai M, Hirose F, Mori S, Yoshimura N. Three-dimensional imaging of macular inner structures in glaucoma by using spectral-domain optical coherence tomography. *Invest Ophthalmol Vis Sci*. 2011;52:1412–1421.
24. Sriram P, Graham SL, Wang C, Yiannikas C, Garrick R, Klistorner A. Transsynaptic retinal degeneration in optic neuropathies: optical coherence tomography study. *Invest Ophthalmol Vis Sci*. 2012;53:1271–1275.
25. Spraul CW, Grossniklaus HE. Vitreous hemorrhage. *Surv Ophthalmol*. 1997;42:3–39.
26. Konstas AG, Hollo G, Astakhov YS, et al. Presentation and long-term follow-up of exfoliation glaucoma in Greece, Spain, Russia, and Hungary. *Eur J Ophthalmol*. 2006;16:60–66.
27. Konstas AG, Jay JL, Marshall GE, Lee WR. Prevalence, diagnostic features, and response to trabeculectomy in exfoliation glaucoma. *Ophthalmology*. 1993;100:619–627.
28. Ritch R, Schlotzer-Schrehardt U. Exfoliation syndrome. *Surv Ophthalmol*. 2001;45:265–315.
29. Mitchell P, Wang JJ, Hourihan F. The relationship between glaucoma and pseudoexfoliation: the Blue Mountains Eye Study. *Arch Ophthalmol*. 1999;117:1319–1324.
30. Johnson TV, Fan S, Camras CB, Toris CB. Aqueous humor dynamics in exfoliation syndrome. *Arch Ophthalmol*. 2008;126:914–920.
31. Campbell DG, Simmons RJ, Grant WM. Ghost cells as a cause of glaucoma. *Am J Ophthalmol*. 1976;81:441–450.
32. Liu L, Wu WC, Yeung L, et al. Ghost cell glaucoma after intravitreal bevacizumab for postoperative vitreous hemorrhage following vitrectomy for proliferative diabetic retinopathy. *Ophthalmic Surg Lasers Imaging*. 2010;41:72–77.
33. Akaishi T, Odani-Kawabata N, Ishida N, Nakamura M. Ocular hypotensive effects of anti-glaucoma agents in mice. *J Ocul Pharmacol Ther*. 2009;25:401–408.
34. Whitlock NA, McKnight B, Corcoran KN, Rodriguez LA, Rice DS. Increased intraocular pressure in mice treated with dexamethasone. *Invest Ophthalmol Vis Sci*. 2010;51:6496–6503.
35. Distelhorst JS, Hughes GM. Open-angle glaucoma. *Am Fam Physician*. 2003;67:1937–1944.
36. Camra CB. Prostaglandins. In: Ritch R, Shields B, Krupin T, eds. *The Glaucomas: Glaucoma Therapy*. Ann Arbor, MI: Mosby; 1996:1449–1461.